Science of the Total Environment 536 (2015) 457–467

Contents lists available at ScienceDirect

Science of the Total Environment

journal homepage: www.elsevier.com/locate/scitotenv

Statistical evaluation of the impact of shale gas activities on ozone pollution in North Texas

Mahdi Ahmadi, Kuruvilla John *

University of North Texas, Denton, TX, USA

HIGHLIGHTS

- The impact of shale gas activities in Barnett Shale on ozone trends was evaluated.
- Raw data analysis shows greater reduction in ozone in the non-shale gas region.
- Meteorological-adjusted ozone time series were developed by KZ-filtering technique.
- M.A. ozone values are higher in areas with shale gas activities.
- Directional analysis shows higher rate of ozone production in the shale gas region.

ARTICLE INFO

Article history:
Received 3 June 2015
Accepted 27 June 2015
Available online 30 July 2015

Editor: D. Barcelo

Keywords:
Shale gas
Hydraulic fracturing
Ozone pollution
Meteorological adjustment
Barnett Shale
Statistical evaluation
Ozone trend

ABSTRACT

Over the past decade, substantial growth in shale gas exploration and production across the US has changed the country's energy outlook. Beyond its economic benefits, the negative impacts of shale gas development on air and water are less well known. In this study the relationship between shale gas activities and ground-level ozone pollution was statistically evaluated. The Dallas–Fort Worth (DFW) area in north-central Texas was selected as the study region. The Barnett Shale, which is one the most productive and fastest growing shale gas fields in the US, is located in the western half of DFW. Hourly meteorological and ozone data were acquired for fourteen years from monitoring stations established and operated by the Texas Commission on Environmental Quality (TCEQ). The area was divided into two regions, the shale gas region (SGR) and the non-shale gas (NSGR) region, according to the number of gas wells in close proximity to each monitoring site. The study period was also divided into 2000–2006 and 2007–2013 because the western half of DFW has experienced significant growth in shale gas activities since 2007. An evaluation of the raw ozone data showed that, while the overall trend in the ozone concentration was down over the entire region, the monitoring sites in the NSGR showed an additional reduction of 4% in the annual number of ozone exceedance days than those in the SGR. Directional analysis of ozone showed that the winds blowing from areas with high shale gas activities contributed to higher ozone downwind. KZ-filtering method and linear regression techniques were used to remove the effects of meteorological variations on ozone and to construct long-term and short-term meteorologically adjusted (M.A.) ozone time series. The mean value of all M.A. ozone components was 8% higher in the sites located within the SGR than in the NSGR. These findings may be useful for understanding the overall impact of shale gas activities on the local and regional ozone pollution.

1. Introduction

The recent expansion of shale gas production has changed the long-term outlook for US energy. Over the recent decade, extraction of natural gas from shale formations has developed rapidly in the USA. Production of natural gas from shale in the USA grew by an average of 17% per year from 2000 to 2006. The successful combination and application of horizontal drilling and high-pressure fracturing in the Barnett Shale, located in the north Texas area accelerated the extraction rate all over the country (Wang and Krupnick, 2013). As a result, US gas production increased 48% annually from 2006 to 2010 (US EIA, 2011). Today, shale gas provides the largest source of growth in the US gas supply. Its share of the total US gas production grew from 1.6% in 2000 to 34% in 2011 (7.85 trillion cubic feet) and is projected to rise to around 50% by 2040 (16.7 trillion cubic feet) (US EIA, 2013). Due to this exponential growth, the United States is expected to become a net exporter of natural gas by 2018 (US EIA, 2014).

* Corresponding author.
E-mail addresses: Mahdi.Ahmadi@unt.edu (M. Ahmadi), Kuruvilla.John@unt.edu (K. John).

http://dx.doi.org/10.1016/j.scitotenv.2015.06.114
0048-9697/

The majority of the growth in shale gas production comes from the geological formations (such as Barnett, Eagle Ford, Bakken, and Marcellus Shale) some of which are close to major urban areas. Therefore, it is necessary to examine the potential impacts of the anthropogenic activities related to shale play on urban and regional environments. One methodological challenge of the current scientific research is the lack of actual measurement baseline data prior to oil and gas development (Moore et al., 2014). Many areas in the proximity of shale gas activities are not equipped with routine air and water quality monitoring system (Carlton et al., 2014). This means that the historical and background data as comparison criteria are rare and it can be a source of controversy (Davies, 2011; Jackson et al., 2011; Osborn et al., 2011; Saba and Orzechowski, 2011; Schon, 2011) that makes science based policy-making difficult (de Melo-Martín et al., 2014; Eaton, 2013; Howarth et al., 2011). Besides, areas such as Dallas–Fort Worth (DFW) have had a long history of air quality problems prior to shale gas development. Therefore, temporal and spatial separation of pollution trends in the area is necessary to evaluate the impact of shale gas activities.

Ground-level ozone (O_3) is a highly reactive chemical species with proven negative impacts on humans, animals, and crops (Koenig, 2000; McKee, 1993; WHO, 2003). Typical activities involved in such unconventional gas development contribute to oxides of nitrogen (NO_X) and volatile organic compound (VOC) emissions (Bar-Ilan et al., 2008; Bunch et al., 2014; Colborna et al., 2014; Gilman et al., 2013; Grant et al., 2009; Litovitz et al., 2013; Pétron et al., 2012; Rich et al., 2014). NO_X is associated with equipment and activities such as drilling, fracking pumps, truck traffic, compressor stations, flaring, and wellhead compressors. In addition to the mentioned sources, VOC emissions are associated with fracking ponds, heaters and dehydrators, blowdown venting, production fugitives, condensate tanks, and pneumatic machineries (Roy et al., 2014). The contribution of one single gas well is trivial when that well is operating properly, but the cumulative impact of thousands of wells on ozone level could be significant. The unprecedented severe wintertime ozone events reported in the Uintah Basin of Utah (Lyman and Shorthill, 2013a; Lyman and Shorthill, 2013b; Martin et al., 2011) and the Upper Green River Basin of Wyoming (Rappenglück et al., 2013; Schnell et al., 2009) (rural areas close to oil and gas production fields) show that when the background ozone is low enough the significance of gas development becomes more obvious. Moreover, numerical modeling of ozone formation and dispersion highlights the possibility of the significant contribution of shale gas activities in near-field and on regional ozone level (Carter and Seinfeld, 2012; Edwards et al., 2013; Kemball-Cook et al., 2010; Mansfield and Hall, 2013; Olaguer, 2012).

Numerical modeling is essential to the understanding of the mechanism of ozone formation and dispersion. However, photochemical modeling is resource intensive and has limitations due to the lack of reliable emission inventories data (the main input of such models). Therefore, as a complementary method, in this work we performed a comprehensive statistical analysis of historical ozone data and constructed meteorologically adjusted (M.A.) ozone time series to evaluate the relationship between shale gas development and ozone pollution in the long-term.

2. Methods

2.1. Study region

DFW is the cultural and economic hub in north Texas. The region's population is estimated at 6.5 million as of July 2011, which makes it the fourth largest metropolitan area in the US, and its 17% annual population growth makes it the fastest growing metropolitan area in the country (U.S. Census Bureau, 2011). With a total area of 9300 mile^2 (24,000 km^2), DFW's urban area is sprawled over 12 counties, 10 out of which have been failing to comply with the National Ambient Air Quality Standards (NAAQS) for ozone set by the US Environmental Protection Agency (EPA) (US EPA, 2013). The DFW ozone problem is driven by the high volume of on-road, off-road and air traffic as well as a variety of small and large point sources. The recent unprecedented emergence of new NO_X and VOC sources from shale gas development activities has potentially added to the air quality burden in the region.

DFW is partially located on the Barnett Shale which is one the most productive and fastest growing shale gas fields in the US. However, shale gas activities have been developed only in the western half of the area due to the geological boundaries of the shale formation. This allows for a clear spatial segregation and makes the comparison between the shale gas region (SGR) and non-shale gas region (NSGR) easier. In addition, this area has been equipped with the air monitoring system by Texas Commission on Environmental Quality (TCEQ) that has been operational over the past three decades; this allows for the evaluation of the long-term impacts on the ozone time series. The study area along with the number of gas wells are shown in Fig. 1.

2.2. Data

Time series of 8-hour average ozone concentrations were extracted from TCEQ's Texas Air Monitoring Information System (TAMISWeb) for the 1997–2014 period from sixteen Continuous Ambient Monitoring Stations (CAMS) operated by TCEQ. The locations of CAMS and the measurement parameters are listed in Table 1. Also the number of gas wells in the 10 mile radial distance of each site at the end of 2013 was calculated with a GIS software and is shown in the same table. It should be noted that some of the monitoring stations were activated past 1997. In addition to the eight-hour (8-hour) averaged measured ozone concentration, 8-hour values of some meteorological variables for the identical period were obtained from the same monitoring sites. Meteorological data include outdoor temperature (T), solar radiation (SR), relative humidity (RH), and wind speed and direction (W).

According to the number of wells as shown in Table 1 we drew a distinction between two regions and named them 'shale gas region' (SGR) and 'non-shale gas region' (NSGR) as two hypothetically separated areas. Such distinction helped the comparison of the local influence of emissions from the shale gas activities on the measured ozone concentration in the region.

2.3. Method of analysis

2.3.1. Statistical evaluation of raw ozone

The trends of simple statistical measures such as ozone design values, number of ozone exceedance days, and the mean value of daily maximum ozone were calculated. Ozone design value is a statistic that corresponds to the ozone status of a given location relative to the level of NAAQS and it is defined as "the 3-year average annual fourth-highest daily maximum 8-hour average ozone concentration." (CFR, 2013). The relationship between raw ozone statistics and meteorological factors were investigated by developing linear correlations between the ozone design values and exceedances and various measures of daily maximum temperature and solar radiation.

2.3.2. Wind effect

The prevailing wind in the study area during the peak ozone season typically blows from the south and the southeast. Thus, the ozone generated in the south-eastern parts of DFW area may be transported to the north-western regions. The general flow direction also coincides with the transport of winds from the NSGR to the SGR. Because the comparison between the two time periods (i.e. before and after 2007) is of interest in this study, wind rose plots for the CAMS were plotted to examine the change in wind direction and speed during the study time periods.

In addition, the relationship between raw ozone changes and wind direction over the study time periods was investigated by using pollution rose diagrams. The ozone concentration data were categorized

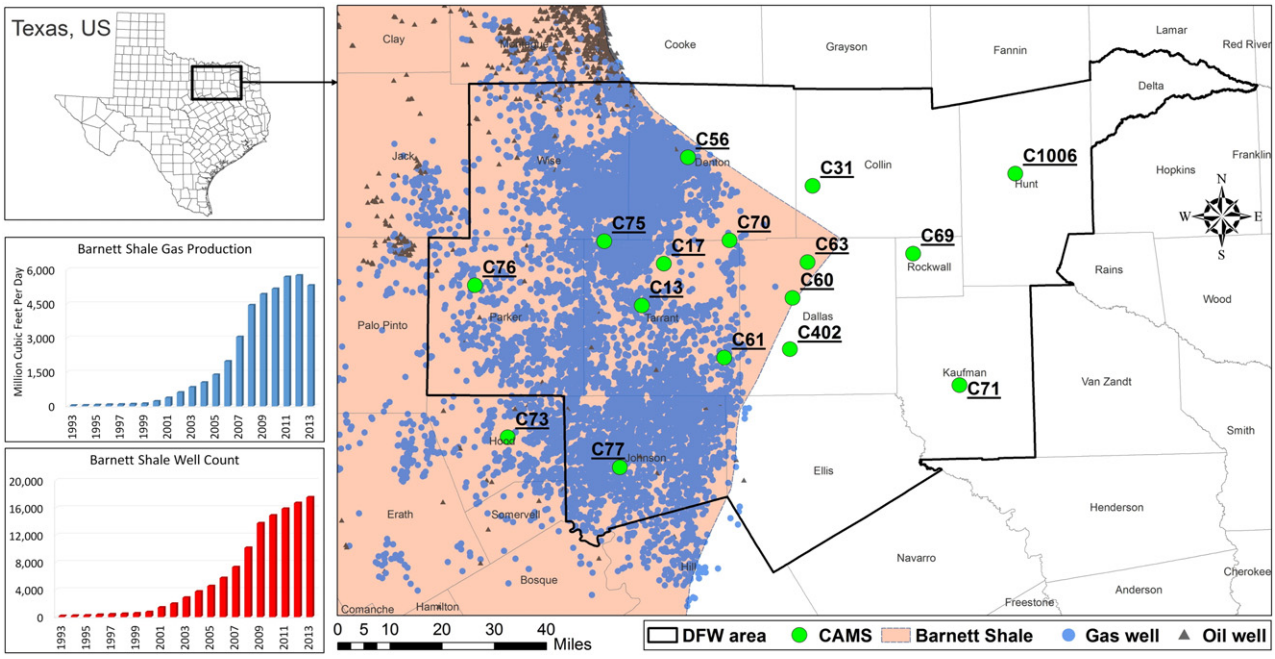

Fig. 1. Study area map with the distribution of on schedule/active wells in the region (RRC, 2014) and the TCEQ's continuous air monitoring stations (CAMS) used in the study (TCEQ, 2014) along with the Barnett Shale well count and natural gas production per day (on the left).

into sixteen compass bins according to the dominant wind direction observed on the same day that the ozone concentration was measured. The resultant numbers for two time periods (before and after 2007) were prepared in a tabular form to evaluate change in the raw ozone concentration within each direction. Ozone variations associated with the wind blowing from the direction with shale gas activities are compared against those directions without shale gas activities upwind. Additionally, the effect of wind is examined by evaluating spatial correlation decay factor which is explained later.

2.3.3. Construction of meteorologically adjusted ozone

Changes in ground-level ozone concentrations greatly depend on the fluctuation of meteorological conditions, particularly solar radiation, outdoor temperature, humidity, and wind (NRC, 1991). Because of the different time scales of physical phenomena embedded in the ozone time series data, spectral decomposition is required to develop meteorologically independent ozone time series.

Table 1
Location of CAMS and parameters used in the study with the total number of gas wells in a 10 mile radial distance of each monitoring site at the end of 2013.

CAMS Code	Location		County	Parameters	No. of wells in 10 mi.
	Lat.	Long.			
C75	32.99	−97.48	Tarrant	O_3, SR, T, W	2723
C77	32.35	−97.44	Johnson	O_3, SR, T, W	1474
C17	32.92	−97.28	Tarrant	O_3, SR, T, W	1364
C56	33.22	−97.20	Denton	O_3, SR, T, RH, W	1362
C13	32.81	−97.36	Tarrant	O_3, SR, T, RH, W	1092
C61	32.66	−97.09	Tarrant	O_3, SR, T, W	862
C73	32.44	−97.80	Hood	O_3, SR, T, W	428
C70	32.99	−97.06	Tarrant	O_3, SR, T, RH, W	299
C76	32.87	−97.91	Parker	O_3, SR, T, W	158
C60	32.82	−96.86	Dallas	O_3, SR, T, RH, W	2
C63	32.92	−96.81	Dallas	O_3, SR, T, W	2
C402	32.68	−96.87	Dallas	O_3, T, W	1
C31	33.13	−96.79	Collin	O_3, SR, T, W	0
C69	32.94	−96.46	Rockwall	O_3, SR, T, W	0
C71	32.56	−96.32	Kaufman	O_3, SR, T, RH, W	0
C1006	33.15	−96.12	Hunt	O_3, SR, T, W	0

In this regard, Rao and Zurbenko's method (Flaum et al., 1996; Rao et al., 1995; Rao and Zurbenko, 1994) was employed in this study to partition the time series of ozone and other meteorological variables. They applied the Kolmogorov–Zurbenko (KZ) filtering method (Zurbenko, 1986) to the time series of ozone and meteorological parameters to separate different components based on their time-scales. Following their method, the application of KZ-filter to each time series can separate them into three components:

$$X(t) = e(t) + S(t) + W(t) \tag{1}$$

where $X(t)$ represents the original time series of a variable, $e(t)$ is the long-term trend component, $S(t)$ is the seasonal component and $W(t)$ is the short-term or stochastic component. In addition, the sum of $e(t)$ and $S(t)$ is denoted as the baseline $BL(t)$, component (Milanchus et al., 1998; Rao et al., 1996, 1997).

KZ-filter is a low-pass filter that can be performed by a simple iterative moving average. It can computationally be defined as k-times application of a centered moving average of $m = 2p + 1$ points over the input time series:

$$Y_i = \frac{1}{m}\sum_{j=-p}^{p} X_{i+j} \tag{2}$$

where X is the original time series and Y is the output time series that becomes the input for the next pass. Therefore the KZ-filter can be written as $KZ_{m,k}(X(t)) = X_{m,k}(t)$ where k is the number of iterations and m is the number of points (days) in the moving average window.

The choice of m and k is critical in determining the cutoff frequency of the filter (Rao et al., 1997). As per earlier studies, the components of the time series can be calculated as:

$$\begin{cases} e(t) = X_{365,3}(\mathrm{t}) \\ S(t) = X_{15,5}(t) - X_{365,3}(t) \\ W(t) = X(t) - X_{15,5}(\mathrm{t}) \\ BL(t) = e(t) + S(t) \end{cases} \tag{3}$$

where variation of $e(t)$ is assumed to be dependent on major climate or pollution policy changes, $S(t)$ strongly depends on seasonal climatic and

emission changes, and $W(t)$ is related to synoptic variation in weather conditions and ozone precursors.

Ozone precursors and meteorological parameters have multiplicative effects in the formation of ozone. The ozone time series should be log-transformed before KZ-filtering that is necessary for effective separation (Rao et al., 1997). As an example, the results of the application of KZ-filter on the log-transformed daily maxima time series of ozone at C56 are presented in Fig. 2. The same type of spectral decomposition was applied to meteorological time series without logarithmic transformation. Because of the centered moving average mechanism and k and m settings for $e(t)$, KZ-filter removed 548 data points (days) from each end of the time series data.

The next step is to calculate the linear regression between the baseline of ozone time series and baseline of meteorological parameters to find the strongest correlations. Also, contribution of each component of KZ-filter to the total variance of the time series is calculated to determine the contribution of each meteorological parameter on the measured ozone concentrations.

After identifying two key parameters that influenced the ozone levels, a three-variable linear regression was developed for each site to calculate the ozone baseline and short-term component as following:

$$O_{BL}(t) = aX_{BL}(t+i) + bY_{BL}(t+j) + c + \epsilon_{BL}(t) \quad (4)$$

$$O_W(t) = aM_W(t) + bN_W(t) + d + \epsilon_W(t) \quad (5)$$

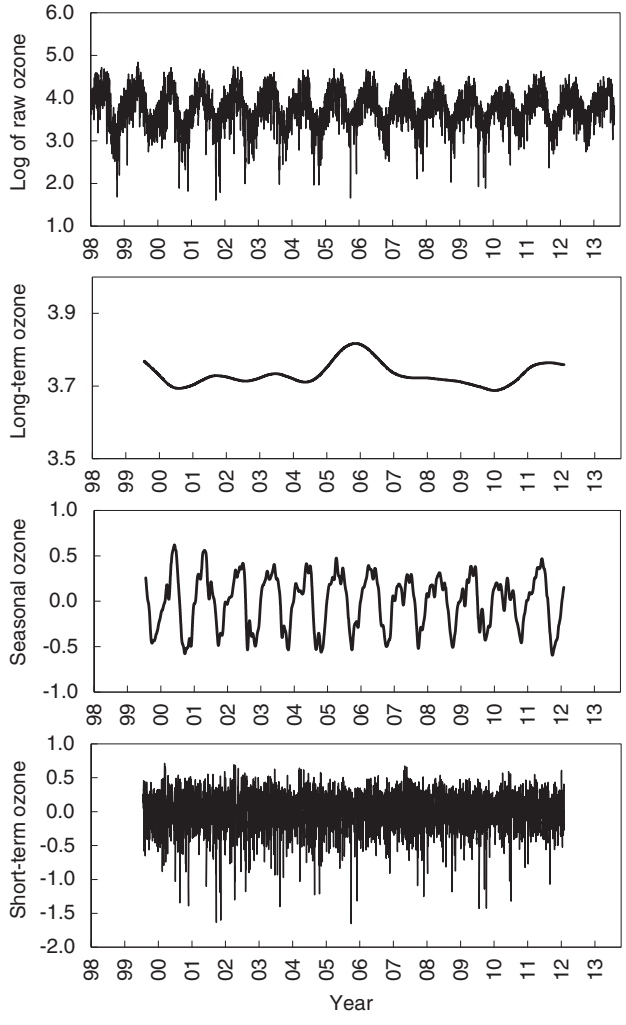

Fig. 2. Daily maxima time series of the natural logarithm of raw ozone (in ppb) at Denton Airport South site (C56) separated by KZ-filter into long-term, seasonal, and short-term.

where a, b, c, and d are fitted parameters, X_{BL} and Y_{BL} are baseline components of two highly correlated meteorological variables (in this study temperature and solar radiation), i and j are number of days each data set was lagged to produce the maximum correlation, M_W and N_W are short-term components of two meteorological variables with the highest correlation with short-term ozone (also, temperature and solar radiation), and $\epsilon_{BL}(t)$ and $\epsilon_w(t)$ are residuals of each regression (the difference between the measured concentrations and the calculated ozone concentrations).

Meteorologically adjusted ozone time series, in which the baseline and short-term effects of meteorological variables are removed as much as possible, was calculated using:

$$O_{\mathrm{MA}}(t) = \epsilon_{\mathrm{BL}}(t) + \epsilon_W(t). \quad (6)$$

Variations in $O_{\mathrm{MA}}(t)$ are mainly due to long-term, seasonal, and short-term fluctuations in ozone precursors. However it includes unexplained meteorological variations due to the limitations of linear regressions in the previous step. The application of KZ-filter one more time on $O_{\mathrm{MA}}(t)$ produces long-term and baseline components that are assumed to be dependent only on the changes in ozone precursors. Therefore both the time series and its long-term components are used to examine the impact of shale gas activities over the long-term.

The short-term component of ozone depends on synoptic fluctuations in weather conditions (particularly wind) and emission sources. Therefore it is used to investigate the impact of wind on the spatial correlation of ozone pollution between the monitoring sites.

2.3.4. Temporal trends of M.A. ozone

The study period was divided into two: first period, 2000–2006 with the development of approximately 700 new wells per year labeled as *B07*, and second, 2007–2013 with 1700 new wells per year across the study area, labeled as *A07*. The trends of raw ozone measured, and the average percent changes were calculated and compared during these two time periods. Also, the trend of M.A. ozone and its components for the study regions and time periods are presented for comparison purpose.

2.3.5. Spatial trends of M.A. ozone

It has been shown that the correlation between the ozone baseline time series at two different locations (at a given time period) decays with distance (Rao et al., 1997). Spatial correlation of short-term components of ozone time series contains information about synoptic influences. Therefore, in addition to the wind rose plots, the impact of wind as a major synoptic variable can be examined by calculating the directional spatial correlation of short-term ozone. It has been shown that there was a strong exponential decay relationship in the correlation between two different monitors and their distance of separation (Rao et al., 1995, 1997). Consequently, along the direction of the prevailing wind, the exponential decay occurs at a lower rate than along all other directions, if the distribution of emission sources were not directionally biased. Therefore, the correlations of the short-term components of ozone time series between different CAMS were calculated along the axes of the prevailing wind (from the south to the north) and perpendicular to it (from the west to the east). The decay factors for each direction were then calculated to examine the impact of wind on the transport of ozone.

3. Results and discussion

3.1. Raw ozone trends

The trends of ozone design values for all CAMS are shown in Fig. 3. Percent change in the design values before and after 2007 varied from site to site. However, the average percent change in the design values

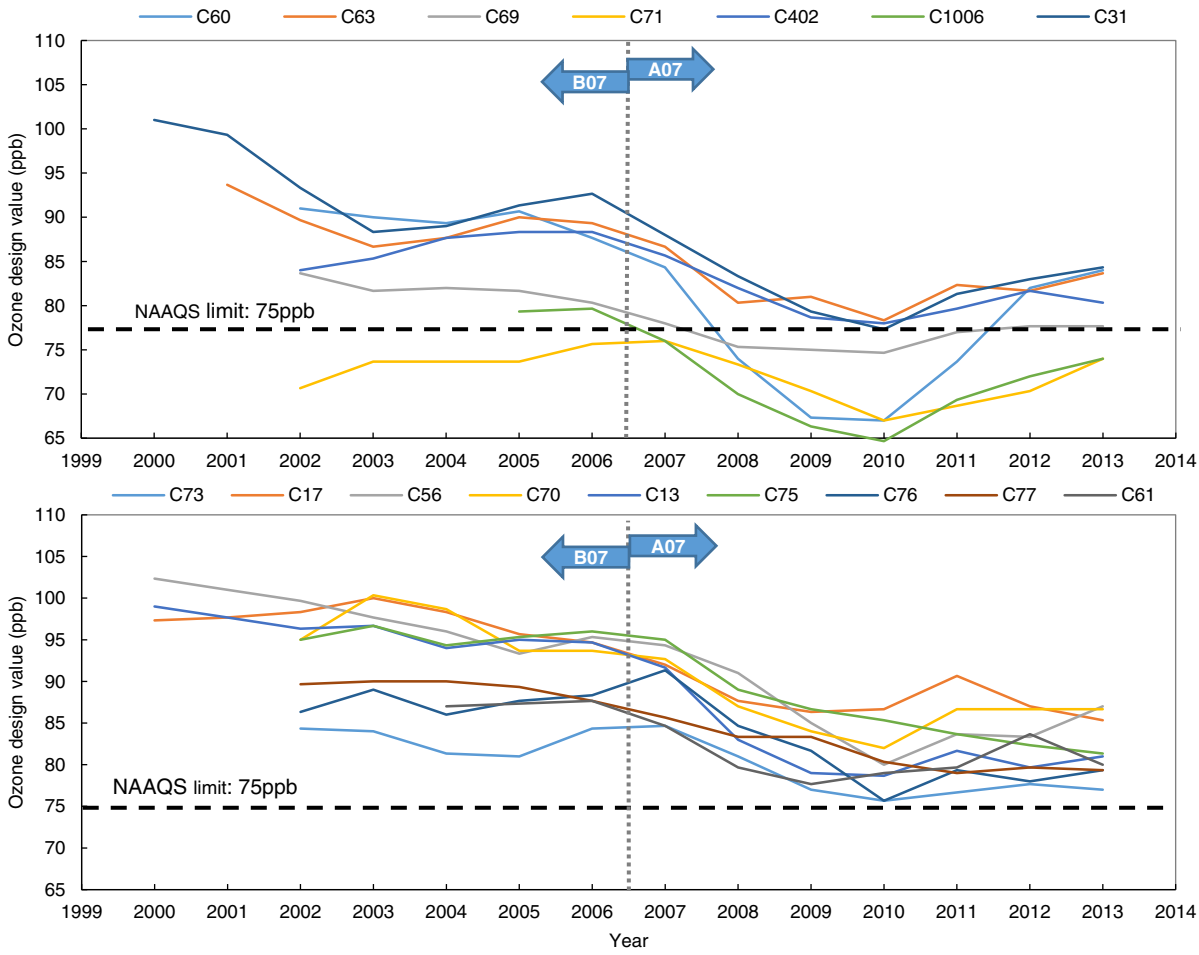

Fig. 3. Trends of ozone design values in NSGR (top) and SGR (bottom) sites.

from 2000–2006 to 2007–2013 was approximately −10%, and was similar for the SGR and NSGR sites.

Because the design values corresponded to the fourth largest values, regression models based on the mean values poorly explain the underlying mechanism. In this regard, extreme value theory that deals with the modeling threshold exceedances is considered to be more useful (Cox and Chu, 1993, 1996; Rao et al., 1992; Smith, 1989; Smith and Huang, 1993). After examining various statistical indicators, such as maximum, mean, median, and percentiles of meteorological parameters, the highest correlation coefficients were achieved when design values were correlated to the three-year average of mean values of the maximum daily temperature and solar radiation for the same month of the year when the fourth highest ozone concentrations were observed. However at all sites, the Pearson product–moment correlation coefficients were negative suggesting that a decrease in the ozone design values was

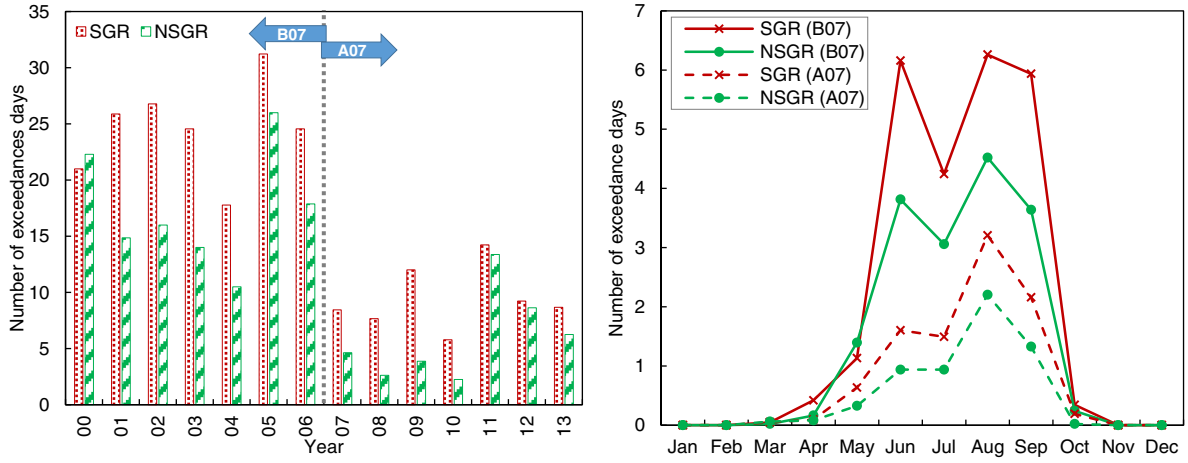

Fig. 4. Number of days with maximum 8-hour ozone concentration exceeding 75 ppb.

associated with a corresponding increase in the temperature and solar radiation.

According to the design value statistics as highlighted in Fig. 3, there was a general downward trend noted at all the sites across the study area prior to 2010. However, after 2010 the trends have shifted upward in almost all of the sites. It was noted that there was no significant difference between the average percent change in the design value trends for the SGR and NSGR sites. However, since 2008 four of the CAMS (C60, C69, C71, and C1006) showed a drop in the design value below the NAAQS (75 ppb); and these CAMS were all located within the NSGR. It is noteworthy that C60 is located within the city of Dallas that has the most land traffic load in the study area. Design values in C1006 and C71 have continued to remain under 75 ppb through 2013.

Annual and monthly trends of the ozone exceedances above the 75 ppb threshold are presented in Fig. 4. The number of exceedance days reduced from B07 to A07 in both the SGR and NSGR, but occurred at different rates. The average percent changes in ozone exceedances from B07 to A07 period were noted to be −61.6% and −65.7% for SGR and NSGR, respectively. During the ozone season (May through September), the reductions observed within the NSGR were about 31% more than within the SGR.

The difference is even larger if the percent reductions are compared on a monthly basis. According to Fig. 4, in NSGR the monthly percent change of exceedances (from B07 to A07) were −78%, −76%, −72%, −54%, and −64% during May, June, July, August, and September, respectively. During the same months, the SGR sites recorded −47%, −74%, −66%, −49%, and −64% reduction, respectively, which are significantly less reductions than in the NSGR especially during May and July. The spatial relationship between the ozone exceedances investigated in other studies show that the correlation is very weak in distances over 15 km (Rao et al., 1997) due to high spatial inhomogeneity of NOx concentration in urban areas. Additionally, shale gas activities introduce many local point sources of VOC and NOx emissions with different intensity and composition at each shale gas site. Therefore, such a significant difference between the SGR and the NSGR sites can be explained in terms of spatial variations of NO_X and VOC that are partly due to an asymmetric spread of industrial shale gas activities over the study area.

3.2. Wind effect

During the ozone seasons, the prevailing wind in the study area blows from south to north. In order to minimize the impact of variation in wind direction on the statistical analysis, wind rose plots for two time period are examined. Figs. 5 and 6 show wind rose plots at the C60 site within the NSGR and the C56 site within the SGR, respectively. It shows that the wind pattern has not changed over the two study time periods.

In the next step, the load of ozone carried by the wind from each direction was examined. Statistical measures of ozone pollution in each wind direction were assessed using pollution rose graphs. For two monitoring stations, the standard compass bins were divided into two groups: directions with and without significant shale gas activities upwind. For the C56 station in Denton city, the upwind wind rose bins highlighting the NNW, N, NNE, NE, ENE, E, and ESE directions were within the NSGR and the remaining bins were within the SGR. For C60 in Dallas, the upwind wind rose bins N, NNE, NE, ENE, E, ESE, SE, SSE, and S bins were within the NSGR and rest of the bins showed winds from the SGR. To evaluate the influence of upwind emission sources on downwind ozone pollution the percent and absolute change of each statistical measure was calculated from the 2000–2006 (B07) period to the 2007–2013 (A07) period.

Results of the directional ozone variation are shown in Table 2. At both sites the changes in the statistical measures are noted to be worse in the direction with the shale gas activity, except for the 90th percentile at the C56 station. That means, from B07 to A07 period higher ozone level was associated with winds that blow from regions with shale gas activities compared to wind blowing from regions without shale gas activities. The higher ozone level probably exists because more sources of ozone precursors exist in the shale gas activities area; this shows a significant negative impact of shale gas activities on downwind raw ozone pollution. More advanced analysis on the spatial correlation of synoptic ozone, as presented in Section 3.5, also support this conclusion.

3.3. Meteorologically adjusted ozone

Following the application of the KZ-filter to all parameters, the square of correlation (R^2) between short-term $W(t)$, long-term $e(t)$, and baseline $BL(t)$ terms were examined to make sure that they are effectively separated ($R^2 < 0.005$). The R^2 between the components of log-transformed ozone and meteorological parameters were calculated. The results are listed in Table 3. The total contribution of each component in the ozone concentrations was calculated by multiplying R^2 with the percent contribution of each component in the total variance of its time series (Rao and Zurbenko, 1994). According to our analysis, there is no need to lag solar radiation time series to maximize the correlation, but temperature time series should be lagged for 6–8 days. This time lag is due to the difference between the peak of ozone and that of the surface temperature (Milanchus et al., 1998). However, the change in R^2 is very small so that the analysis can be done without lagging the time series.

Table 3 shows that solar radiation and temperature have the highest correlations with both ozone baseline and short-term components. Consequently, these two parameters have the largest contribution in

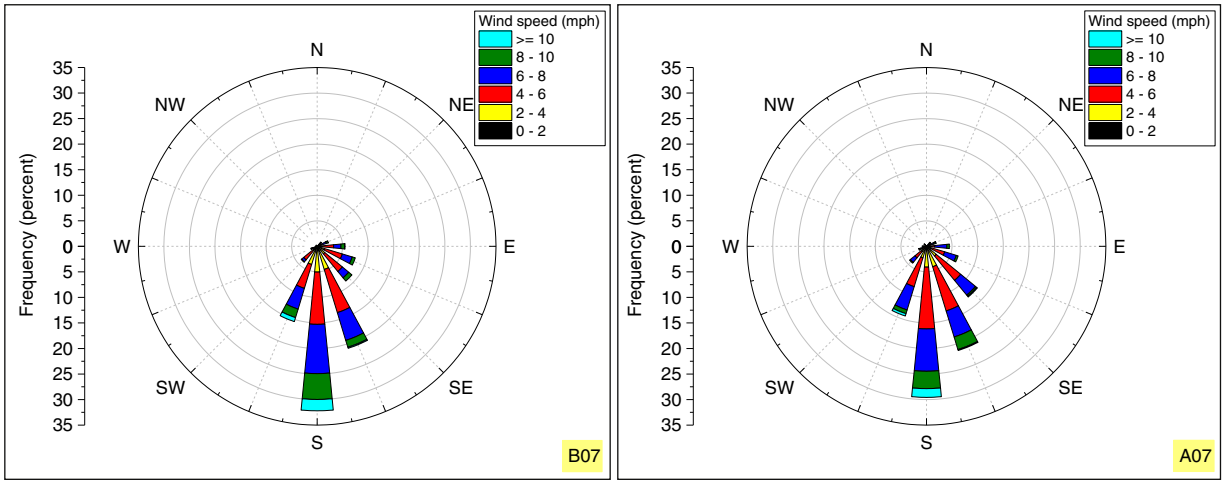

Fig. 5. Wind rose at Dallas Hinton St. (C60) before 2007 (left) and after 2007 (right).

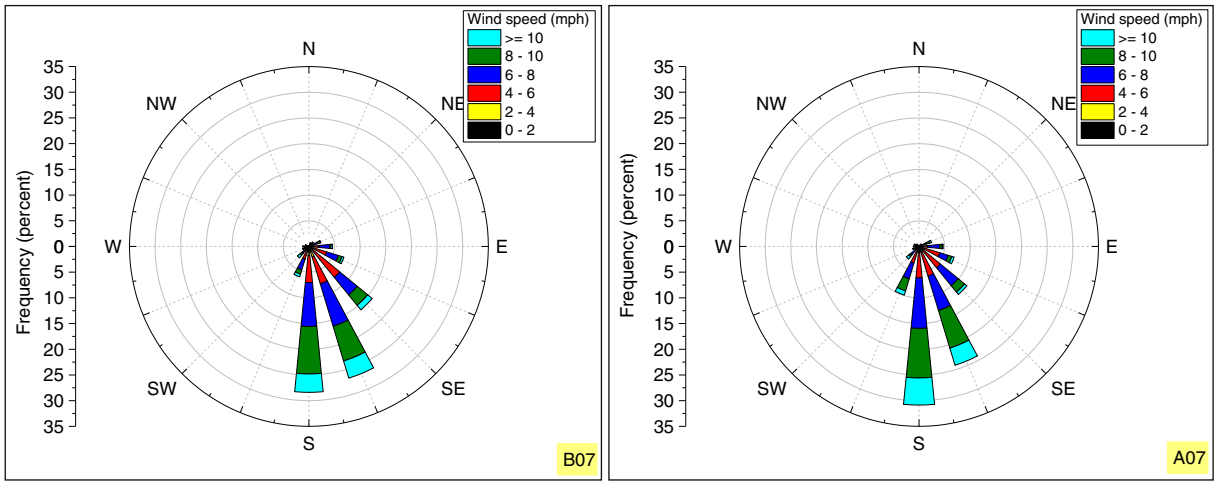

Fig. 6. Wind rose at Denton Airport South (C56) before 2007 (left) and after 2007 (right).

the short-term and baseline ozone concentrations. Therefore, solar radiation and outdoor temperature were employed to calculate meteorologically adjusted (M.A.) ozone. By means of these two parameters approximately 83 to 91% of ozone concentration variation can be explained. It is important to note that meteorological factors do not produce ozone independently. Rather they modulate the effect of ozone precursors emitted from the sources into the ambient (Milanchus et al., 1998). Residuals of the linear regression represent M.A. ozone. By the second application of the KZ-filter on residuals, long-term, baseline and short-term components of M.A. ozone can be separated. Fig. 7 shows M.A. ozone results for two of the monitoring stations.

3.4. M.A. ozone trends

Using the M.A. ozone ($O_{M.A.}$) time series, annual mean $\bar{O}_{M.A.}$, median, maximum, minimum, and first and third quartiles were calculate for each site. The results for the SGR and the NSGR are presented in Fig. 8. It should be noted that because all values are expressed as the natural logarithm of the raw ozone data, M.A. ozone values (and hence $\bar{O}_{M.A.}$), have multiplicative effect in the original time series. Also because $O_{M.A.}$ values are sufficiently small it follows:

$$\exp(O_{M.A.}) \approx 1 + O_{M.A.}. \quad (7)$$

Therefore, in Fig. 8, $\bar{O}_{M.A.} \times 100$ values represent the percent change in the mean value of the original raw ozone time series. Consequently, the negative values mean decrease in concentration from the mean value of the total ozone time series (Rao and Zurbenko, 1994).

Fig. 8 demonstrates the rise in M.A. ozone statistics within the SGR after 2008, while over the same time period there M.A. ozone has been decreased within the NSGR. One important reason for the difference in the trends is probably the variations in the ozone precursors. Figs. 9 and 10 show box plots of VOC and NO_X in two monitoring sites: C56 is located in the SGR and C60 is within the NSGR. Since 2011 TCEQ operated canisters collected air samples that were then analyzed for VOC in the TCEQ laboratory. The concentrations were quantified for a total of 45 VOC species. The trends in Fig. 8 shows a significant increase in the 99th percentile, maximum and mean VOC concentrations at the Denton Airport South (C56) while it remains steady at the C60 site. High VOC concentrations can contribute to higher hourly ozone, whereas an increase in the mean value of VOC has long-term effect on the ozone trend. This could be a result of shale gas activities around the Denton site as in the different stages VOC are vented or leaked from facilities and devices associated with oil and gas exploration activities. Fig. 9 shows that at both sites there was a similar increase in the NO_X concentration and the rate of change was not notably different.

The M.A. ozone time series contain information of both ozone precursors and unexplained meteorological variations. Although the share of unexplained climatic factors is minimal in this study but removing the remaining of meteorological information from M.A. ozone time series is useful. By applying the KZ-filter one more time, the long-term component of M.A. ozone can be separated which is assumed to be entirely meteorology independent. The only problem is with removing unexplained synoptic and seasonal components, we actually remove seasonal and synoptic emission information as well. That is, long-term M.A. ozone cannot account for seasonal and synoptic changes in ozone precursors while some emission sources have synoptic and seasonal behavior. Therefore all components of M.A. ozone should be examined to address spatial and temporal changes in the emission distribution.

Table 2
Effect of shale gas activities on downwind ozone pollution from 2006–2007 (B07) to 2007–2013 (A07) in two directions SGR and NSGR.

Parameter	C60 station				C56 station			
	Absolute change (ppb)		Percent change		Absolute change (ppb)		Percent change	
	SGR	NSGR	SGR	NSGR	SGR	NSGR	SGR	NSGR
Max	1.1	−12.1	1.7%	−13.4%	−1.6	−4.4	−1.9%	−5.8%
99th percentile	−0.6	−7.5	−0.9%	−9.6%	−2.7	−4.9	−3.5%	−6.8%
90th percentile	1.0	−6.0	2.1%	−9.4%	−4.2	−2.1	−6.7%	−3.5%
75th percentile	3.7	−4.3	9.8%	−8.2%	−1.3	−2.2	−2.5%	−4.4%
Median	4.4	0.6	15.3%	1.6%	0.7	−0.5	1.8%	−1.3%
Mean	3.7	−0.6	12.4%	−1.6%	−0.4	−0.8	−1.0%	−2.0%
25th percentile	4.6	2.2	21.3%	8.5%	0.7	0.5	2.1%	1.7%
10th percentile	5.2	4.8	33.5%	27.7%	1.2	−0.4	4.7%	−1.8%
1st percentile	3.0	3.0	37.3%	32.7%	1.8	0.6	12.0%	4.1%
Min	3.8	1.4	63.1%	21.3%	0.4	−0.3	3.2%	−1.9%

Table 3
Square of correlation coefficient (R^2) between (a) baseline of ozone and baseline meteorological variables (T: temperature, SR: solar radiation, RH: relative humidity, WS: wind speed); and (b) short-term ozone and short-term meteorological variables; and percent contribution of each variable in ozone.

CAMS	R^2				Percent contribution (%)			
	T	SR	RH	WS	T	SR	RH	WS
Baseline								
C76	0.78	0.81	–	0.21	28	29	–	8
C73	0.80	0.83	–	0.10	28	29	–	4
C75	0.78	0.79	–	0.22	33	33	–	9
C77	0.80	0.85	–	0.12	30	32	–	5
C13	0.75	0.83	0.04	0.18	32	36	2	8
C17	0.73	0.77	–	0.15	35	37	–	7
C56	0.72	0.76	0.03	0.10	36	38	2	5
C61	0.73	0.86	–	0.12	27	32	–	4
C70	0.71	0.79	0.02	0.17	31	35	1	7
C402	0.79	0.80	–	0.20	33	34	–	8
C60	0.73	0.80	0.02	0.13	35	38	1	6
C63	0.72	0.79	–	0.14	36	40	–	7
C31	0.73	0.76	–	0.10	38	40	–	5
C69	0.77	0.81	–	0.18	32	33	–	7
C71	0.80	0.86	0.03	0.14	30	33	1	5
C1006	0.81	0.85	–	0.16	31	32	–	6
Short-term								
C76	0.17	0.32	–	0.00	10	18	–	0
C73	0.12	0.39	–	0.00	7	23	–	0
C75	0.08	0.30	–	0.00	4	16	–	0
C77	0.16	0.34	–	0.00	9	19	–	0
C13	0.13	0.23	0.05	0.00	7	12	3	0
C17	0.08	0.32	–	0.00	4	15	–	0
C56	0.10	0.25	0.03	0.00	4	11	1	0
C61	0.11	0.33	–	0.00	6	18	–	0
C70	0.15	0.27	0.05	0.00	8	14	3	0
C402	0.11	0.30	–	0.00	6	15	–	0
C60	0.10	0.26	0.04	0.00	5	12	2	0
C63	0.11	0.22	–	0.00	5	10	–	0
C31	0.10	0.26	–	0.00	4	11	–	0
C69	0.12	0.31	–	0.00	6	16	–	0
C71	0.15	0.30	0.06	0.00	8	17	3	0
C1006	0.09	0.35	–	0.00	5	19	–	0

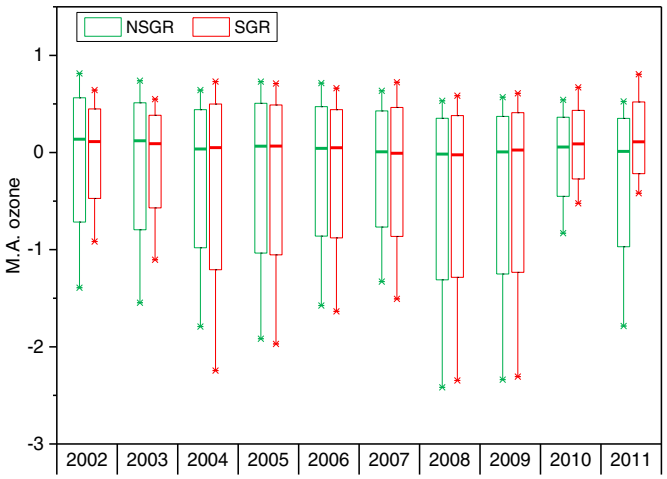

Fig. 8. Box plot of M.A. ozone concentrations over the DFW area. The maximum, the 75th percentile, the median, the 25th percentile, and the minimum are shown.

Figs. 11 through 13 show sudden changes in the M.A. ozone trends at all the monitoring sites across the study region. The reversal of trends in the M.A. ozone time series after 2008 is in agreement with the change in the ozone design value trends as reflected by the three-year average statistics. However, the sites within the SGR show significantly larger increases in the M.A. ozone statistical measures (Figs. 11, 12, and 13). Any increase in the M.A. ozone can potentially lead to higher ozone level if the meteorological factors favor ozone photochemical reactions. This may be the cause of higher ozone exceedances in the SGR compared to the NSGR. With the continuation of the current upward trend within SGR into the future years, cities in the SGR or downwind will have more ozone exceedances assuming that there will be no major temperature change over the future ozone season.

In addition to higher M.A. ozone levels within the SGR, it is noticeable that there was a divergence in the trends noted within the SGR

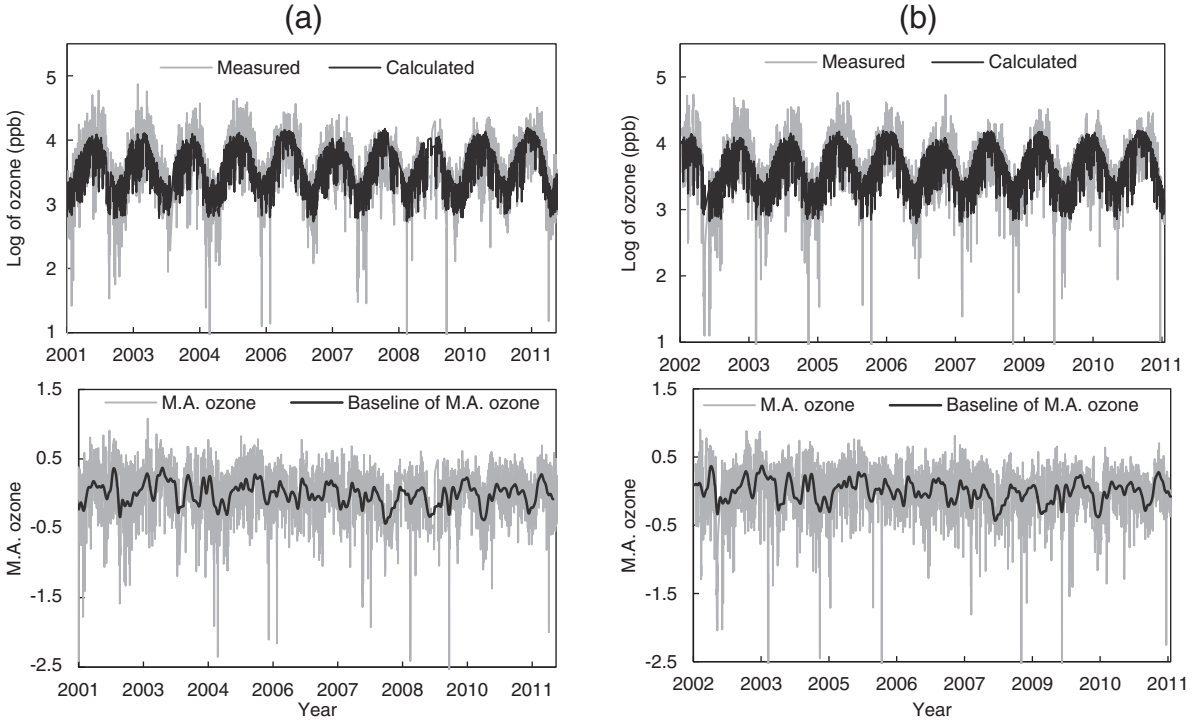

Fig. 7. Daily maxima time series of the measured and calculated natural logarithm of ozone; meteorologically adjusted ozone time series and its baseline component at (a) Dallas Hinton St. (C60), and (b) Denton Airport South (C56).

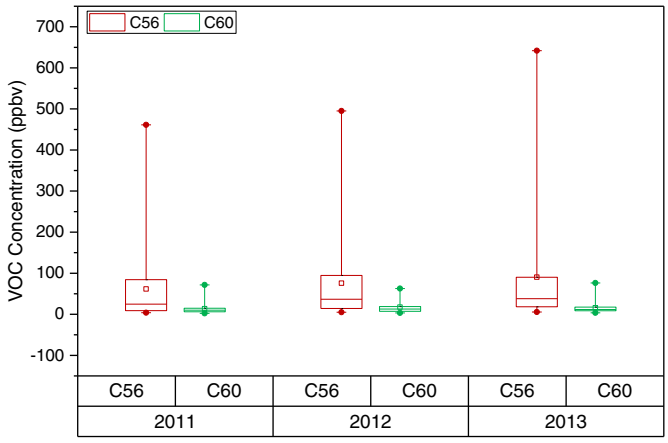

Fig. 9. Box plot of VOC concentrations at Denton Airport South (C56) and Dallas Hinton St. (C60). The maximum, the 75th percentile, the median, the 25th percentile, and the minimum are shown.

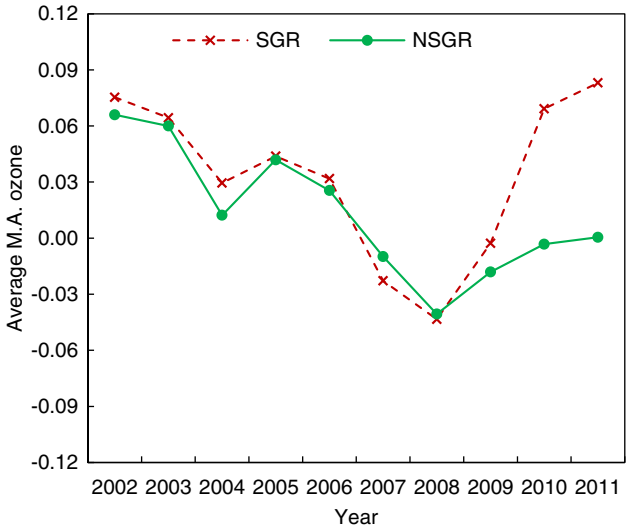

Fig. 11. Trends of mean value of M.A. ozone.

and the NSGR after 2008. This local divergence on a small spatial scale (compared to the meteorological spatial scale) may be caused by directionally biased distribution of emission sources. The time of the change in the distribution of emission sources correlates with the second time period (2007–2013) where the number of wells per year was significantly higher than the first time period. In other words, faster growth in the number of shale wells correlates well with the increase in anthropogenic ozone in the SGR. Changes in the long-term trend (Fig. 13) that are supposed to be entirely independent of meteorological variables, clearly shows the influence of the increase in the local ozone precursor emissions.

3.5. Spatial decay analysis

Spatial behavior of ozone can be investigated using graphs of correlation coefficients between different sites as a function of distance. If the correlation coefficients are calculated between short-term ozone at different sites, then the graph would contain information about wind as major synoptic parameter (Rao et al., 1997). Correlation coefficients between a base site C13 (located within the SGR) and other sites in two normal directions were calculated. The major axis is the direction along the prevailing wind measured at the base site and the minor axis is perpendicular to that. Therefore, differences between correlation coefficient decay graphs in two normal directions represent the differences between synoptic ozone behaviors along those directions. Similar calculations are performed for C60 (located in NSGR) and the results are presented in Fig. 14.

The graphs of the exponential decay of spatial correlation between short-term ozone in different locations show that along the direction of prevailing wind, the correlation coefficient decays as fast as in the direction normal to the prevailing wind. In the case of the C60 monitor (Dallas Hinton St.) the correlation decays even faster along the wind direction. This is counter to the findings from earlier studies (Rao et al., 1997) because spatial correlation along the major wind direction should be stronger due to the transport and dispersion of ozone. One plausible explanation for this is, that there could be significant ozone sources or sinks (due to titration as a result of high NO concentration) along the path of the prevailing wind. In either case, as shown in Fig. 14 the distribution of NO_X and VOC sources is directionally biased because if they were distributed evenly one would have observed a slower decay along the direction of the prevailing wind.

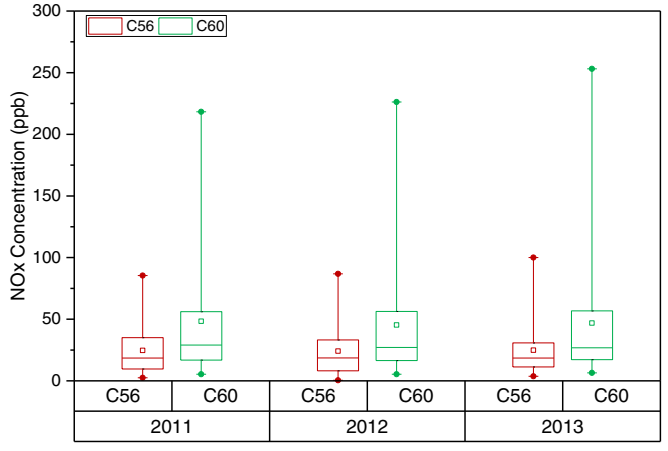

Fig. 10. Box plot presentation of daily 1-hour maximum NO_X statistics in Denton Airport South (C56) and Dallas Hinton St. (C60).

4. Conclusion

In this research the long-term trends of measured ozone concentrations within the Dallas–Fort Worth area were evaluated using over 14 years of data obtained from TCEQ. The study area was divided into

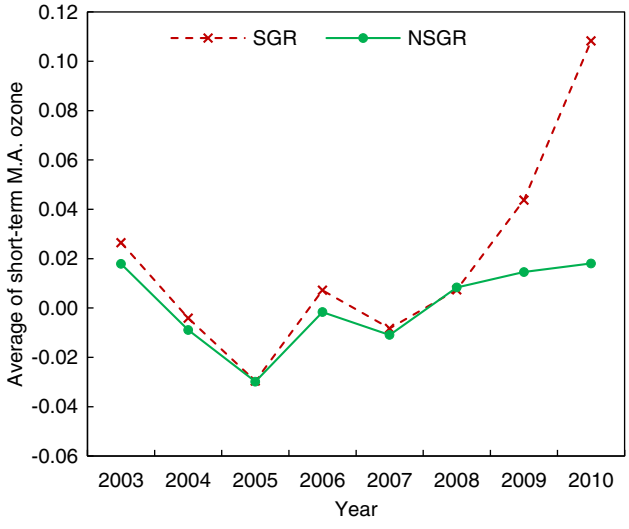

Fig. 12. Annual mean value of short-term component of M.A. ozone.

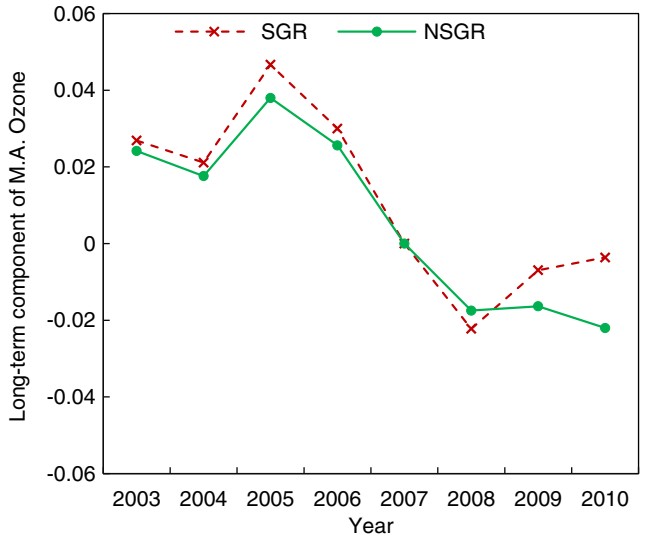

Fig. 13. Annual mean value of long-term component of M.A. ozone.

two hypothetical regions to evaluate the effect of oil and gas activities within the Barnett Shale. The trends were studied and compared over two time periods, from 2000 to 2006 (B07) and from 2007 to 2013 (A07), as the volume of shale gas production and gas well numbers showed a significant increase since 2007. The results of the first part of the analysis show that the sites within the non-shale gas region (NSGR) showed a larger decrease in the number of ozone exceedances than at sites located within the shale gas region (SGR). The average percent changes in ozone exceedances from B07 to A07 period were −61.6% and −65.7% in the SGR and the NSGR, respectively. During the high ozone season, the maximum reduction rate within the NSGR was about 31% more than within the SGR.

In the second part of the study, the KZ-filtering method and linear regression were used to construct meteorologically adjusted (M.A.) ozone time series. The statistical analysis of M.A. ozone was in agreement with the findings shown in the first part. After 2008, there was an unprecedented increase in the statistical parameters of M.A. ozone within the SGR, because the mean value of the long-term component of M.A. ozone was 2% higher than within the NSGR. The mean value of short-term M.A. ozone was almost 10% higher within the SGR than within the NSGR. The average of all M.A. ozone components was about 8% higher within the SGR than in the NSGR. VOC concentration data collected at two of the monitoring sites show very sharp upward trend in the mean and peak values in the site located within the SGR. The analysis of the wind data showed no significant change in the wind pattern at all sites. Furthermore, the spatial decay analysis of the short-term ozone correlations at different locations show that the emission sources tended to be directionally biased. Within the study area, the major source of asymmetry was attributed to the distribution of VOC and NO_X emission sources associated with shale gas activities.

The statistical analyses presented in this work strongly support the idea of temporal and spatial connection between shale gas activities and changes in the long-term ozone trends within the Dallas–Fort Worth area. Further research including photochemical modeling and near-site measurements are recommended to facilitate better understanding of the relationship between ozone pollution and oil and gas activities.

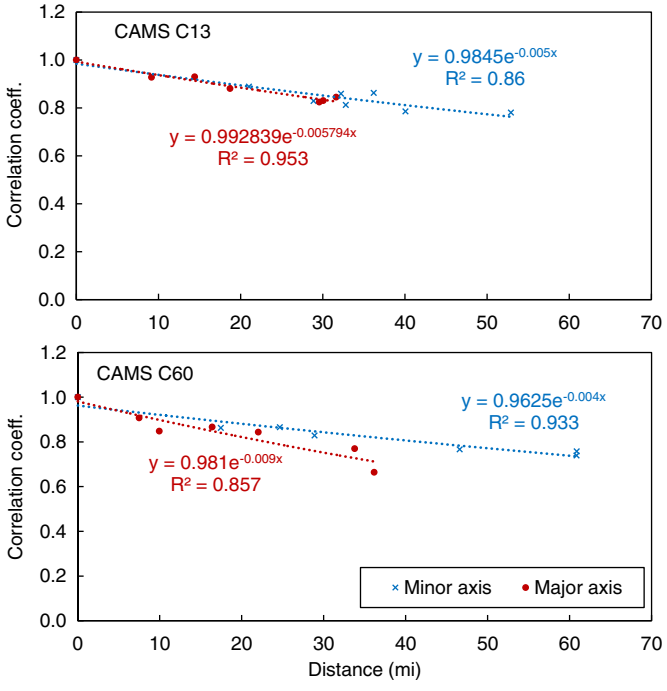

Fig. 14. Correlation coefficient as a function of distance from three monitoring sites between short-term ozone in the direction of the prevailing wind (major axis), and along the direction normal to the prevailing wind (minor axis).

Acknowledgments

The authors would like to thank the Railroad Commission of Texas (RRC), Austin, Texas, for providing data on oil and gas wells. We would also like to thank the Texas Commission on Environmental Quality (TCEQ) for providing access to the air quality data used in this study. We would like to thank the reviewers for providing insightful comments and feedback on this manuscript.

References

Bar-Ilan, A., Grant, J., Friesen, R., Pollack, A.K., 2008. Development of Baseline 2006 Emissions from Oil and Gas Activity in the Denver-Julesburg Basin Prepared for. Colorado Department of Public Health and Environment Air Pollution Control Division, Novato, CA.

Bunch, A.G., Perry, C.S., Abraham, L., Wikoff, D.S., Tachovsky, J.A., Hixon, J.G., et al., 2014. Evaluation of impact of shale gas operations in the Barnett Shale region on volatile organic compounds in air and potential human health risks. Sci. Total Environ. 468, 832–842.

Carlton, A.G., Little, E., Moeller, M., Odoyo, S., Shepson, P.B., 2014. The data gap: can a lack of monitors obscure loss of clean air act benefits in fracking areas? Environ. Sci. Technol. 48, 893–894.

Carter, W.P., Seinfeld, J.H., 2012. Winter ozone formation and VOC incremental reactivities in the Upper Green River Basin of Wyoming. Atmos. Environ. 50, 255–266.

CFR, 2013. Title 40 — Protection of Environment: 40 CFR Part 50 — Appendix I: Interpretation of the 8-hour Primary and Secondary National Ambient Air Quality Standards for Ozone. U.S. Government Printing Office, Washington, DC.

Colborna, T., Schultza, K., Herricka, L., Kwiatkowskia, C., 2014. An exploratory study of air quality near natural gas operations. J. Air Waste Manage. Assoc. 20, 86–105.

Cox, W.M., Chu, S.-H., 1993. Meteorologically adjusted ozone trends in urban areas: a probabilistic approach. Atmos. Environ. B Urban Atmos. 27, 425–434.

Cox, W.M., Chu, S.-H., 1996. Assessment of interannual ozone variation in urban areas from a climatological perspective. Atmos. Environ. 30, 2615–2625.

Davies, R.J., 2011. Methane contamination of drinking water caused by hydraulic fracturing remains unproven. Proc. Natl. Acad. Sci. 108, E871.

de Melo-Martín, I., Hays, J., Finkel, M.L., 2014. The role of ethics in shale gas policies. Sci. Total Environ. 470, 1114–1119.

Eaton, T.T., 2013. Science-based decision-making on complex issues: Marcellus shale gas hydrofracking and New York City water supply. Sci. Total Environ. 461–462, 158–169.

Edwards, P.M., Young, C.J., Aikin, K., deGouw, J., Dubé, W.P., Geiger, F., et al., 2013. Ozone photochemistry in an oil and natural gas extraction region during winter: simulations of a snow-free season in the Uintah Basin, Utah. Atmos. Chem. Phys. 13, 8955–8971.

Flaum, J.B., Rao, S.T., Zurbenko, I.G., 1996. Moderating the influence of meteorological conditions on ambient ozone concentrations. J. Air Waste Manage. Assoc. 46, 35–46.

Gilman, J.B., Lerner, B.M., Kuster, W.C., de Gouw, J.A., 2013. Source signature of volatile organic compounds from oil and natural gas operations in Northeastern Colorado. Environ. Sci. Technol. 47, 1297–1305.

Grant, J., Parker, L., Bar-Ilan, A., Kemball-Cook, S., Yarwood, G., 2009. Development of Emissions Inventories for Natural Gas Exploration and Production Activity in the Haynesville Shale, Novato, CA.

Howarth, R.W., Ingraffea, A., Engelder, T., 2011. Natural gas: should fracking stop? Nature 477, 271–275.

Jackson, R.B., Osborn, S.G., Vengosh, A., Warner, N.R., 2011. Reply to Davies: hydraulic fracturing remains a possible mechanism for observed methane contamination of drinking water. Proc. Natl. Acad. Sci. 108, E872.
Kemball-Cook, S., Bar-Ilan, A., Grant, J., Parker, L., Jung, J., Santamaria, W., et al., 2010. Ozone impacts of natural gas development in the Haynesville shale. Environ. Sci. Technol. 44, 9357–9363.
Koenig, J.Q., 2000. Health Effects of Ambient Air Pollution: How Safe Is the Air We Breathe? Springer
Litovitz, A., Curtright, A., Abramzon, S., Burger, N., Samaras, C., 2013. Estimation of regional air-quality damages from Marcellus Shale natural gas extraction in Pennsylvania. Environ. Res. Lett. 8, 014017.
Lyman, S., Shorthill, H., 2013a. Final Report: 2012 Uinta Basin Winter Ozone and Air Quality Study. Office of Commercialization and Regional Development, Utah State University, Logan, UT.
Lyman, S., Shorthill, H., 2013b. Final Report: 2013 Uinta Basin Winter Ozone and Air Quality Study. Office of Commercialization and Regional Development, Utah State University, Logan, UT.
Mansfield, M., Hall, C., 2013. Statistical analysis of winter ozone events. Air Qual. Atmos. Health 6, 687–699.
Martin, R., Moore, K., Mansfield, M., Hill, S., Harper, K., Shorthill, H., 2011. Final Report: Uinta Basin Winter Ozone and Air Quality Study: December 2010 - March 2011. Energy Dynamics Laboratory, Utah State University Research Foundation, Vernal, UT.
McKee, D., 1993. Tropospheric Ozone: Human Health and Agricultural Impacts. CRC Press.
Milanchus, M.L., Rao, S.T., Zurbenko, I.G., 1998. Evaluating the effectiveness of ozone management efforts in the presence of meteorological variability. J. Air Waste Manage. Assoc. 48, 201–215.
Moore, C.W., Zielinska, B., Petron, G., Jackson, R.B., 2014. Air impacts of increased natural gas acquisition, processing, and use: a critical review. Environ. Sci. Technol. 48 (15), 8349–8359.
NRC. (National Research Council. Committee on Tropospheric Ozone Formation Measurement), 1991. Rethinking the Ozone Problem in Urban and Regional Air Pollution. National Academy Press.
Olaguer, E.P., 2012. The potential near-source ozone impacts of upstream oil and gas industry emissions. J. Air Waste Manage. Assoc. 62, 966–977.
Osborn, S.G., Vengosh, A., Warner, N.R., Jackson, R.B., 2011. Methane contamination of drinking water accompanying gas-well drilling and hydraulic fracturing. Proc. Natl. Acad. Sci. 108, 8172–8176.
Pétron, G., Frost, G., Miller, B.R., Hirsch, A.I., Montzka, S.A., Karion, A., et al., 2012. Hydrocarbon emissions characterization in the Colorado Front Range: a pilot study. J. Geophys. Res. 117, D04304.
Rao, S.T., Zurbenko, I.G., 1994. Detecting and tracking changes in ozone air quality. Air waste 44, 1089–1092.
Rao, S.T., Sistla, G., Henry, R., 1992. Statistical analysis of trends in urban ozone air quality. J. Air Waste Manage. Assoc. 42, 1204–1211.
Rao, S.T., Zalewsky, E., Zurbenko, I.G., 1995. Determining temporal and spatial variations in ozone air quality. J. Air Waste Manage. Assoc. 45, 57–61.
Rao, S.T., Zurbenko, I., Porter, P., Ku, J., Henry, R., 1996. Dealing with the ozone non-attainment problem in the Eastern United States. Environ. Manag. 1, 17–31.
Rao, S.T., Zurbenko, I., Neagu, R., Porter, P., Ku, J., Henry, R., 1997. Space and time scales in ambient ozone data. Bull. Am. Meteorol. Soc. 78, 2153–2166.
Rappenglück, B., Ackermann, L., Alvarez, S., Golovko, J., Buhr, M., Field, R., et al., 2013. Strong wintertime ozone events in the Upper Green River Basin, Wyoming. Atmos. Chem. Phys. Discuss. 13, 17953–18005.
Rich, A., Grover, J.P., Sattler, M.L., 2014. An exploratory study of air emissions associated with shale gas development and production in the Barnett Shale. J. Air Waste Manage. Assoc. 64, 61–72.
Roy, A.A., Adams, P.J., Robinson, A.L., 2014. Air pollutant emissions from the development, production, and processing of Marcellus Shale natural gas. J. Air Waste Manage. Assoc. 64, 19–37.
RRC. (The Railroad Commission of Texas), 2014. Barnett Shale Information. Railroad Commission of Texas.
Saba, T., Orzechowski, M., 2011. Lack of data to support a relationship between methane contamination of drinking water wells and hydraulic fracturing. Proc. Natl. Acad. Sci. 108, E663.
Schnell, R.C., Oltmans, S.J., Neely, R.R., Endres, M.S., Molenar, J.V., White, A.B., 2009. Rapid photochemical production of ozone at high concentrations in a rural site during winter. Nat. Geosci. 2, 120–122.
Schon, S.C., 2011. Hydraulic fracturing not responsible for methane migration. Proc. Natl. Acad. Sci. 108, E664.
Smith, R.L., 1989. Extreme value analysis of environmental time series: an application to trend detection in ground-level ozone. Stat. Sci. 4, 367–377.
Smith, R.L., Huang, L.-S., 1993. Modeling High Threshold Exceedances of Urban Ozone. National Institute of Statistical Sciences.
TCEQ, 2014. Site List. Texas Commission on Environmental Quality.
U.S. Census Bureau, 2011. Metropolitan and Micropolitan Statistical Areas Totals: Vintage 2011 Retrieved from, http://www.census.gov/popest/data/metro/totals/2011/index.html (access: April 8, 2015).
US EIA, 2011. Annual Energy Outlook 2011 with Projections to 2035. Energy Information Administration, United States Department of Energy, Washington DC.
US EIA, 2013. Annual Energy Outlook 2013 with Projections to 2040. Energy Information Administration, United States Department of Energy, Washington DC.
US EIA, 2014. AEO2014 Early Release Overview. Energy Information Administration, United States Department of Energy.
US EPA, 2013. Nonattainment Status for Each County by Year for Texas Including Previous 1-Hour Ozone Counties.
Wang, Z., Krupnick, A., 2013. A retrospective review of shale gas development in the United States. Resources for the Future Discussion Paper.
WHO, 2003. Health Aspects of Air Pollution With Particulate Matter, Ozone and Nitrogen Dioxide: Report on a WHO Working Group. World Health Organization, Regional Office for Europe.
Zurbenko, I.G., 1986. The Spectral Analysis of Time Series. North-Holland.